Electronic Supplementary Material (ESI) for Nanoscale.

Hand-Crafted Potent Hydroxyl-rich Husk Succoured Fe_3O_4 @ Cu, Mn, Ni, Co –Tetra-metallic Heterogenous Nanocomposite as Catalytic Accelerant

Ramya Ravichandran[a], Arun Annamalai [a], Kumaresan Annamalai [a], Anandhavalli Jeevarathinam [a], Suresh Ranganathan[b], Sundaravadivel Elumalai [a] *

[a] Department of Chemistry, SRM Institute of Science and Technology, Kattankulathur, Tamil Nadu – 603 203, India.

[b] Department of Chemistry, Centre for Material Chemistry, Karpagam Academy of Higher Education, Coimbatore – 641021, India.

*Corresponding Author E-mail: sundaravadivelchem@gmail.com

1. Experimental section

1.1 Preparation of Hydroxyl-rich Oryza Sativa Husk

The husk (OSH) was collected after the reaping of paddy from the fields. The collected husk had been washed with ethanol-water mixture and then it is dried under oven at 60 ºC overnight for 6 hours. The dried husk was then grind into smaller fragments using mortar and pestle. Then the OSH is subjected to sieve under 4 µm pore-sized sieve cloth membrane. The resultant OSH powder passed through the membrane was collected, stored, and used for further preparation of the nanocomposite.

2. Scavenger Studies for the OSFTC

The photocatalytic activity was conducted, and an analysis was undertaken to determine whether any of the generated radicals played a significant role in degrading the pollutant during the reaction. This was verified through scavenging studies (Fig.S6 -a). In the visible-light-driven reaction, photoactive species such as superoxide radicals ($\bullet O_2^-$), hydroxyl radicals (•OH), electrons (e^-), and holes (h^+) were involved. Among these generated species, we suppressed one of them and conducted the reaction to analyse the impact caused by the remaining species. 1,4-benzoquinone, ethylenediaminetetraacetic acid (EDTA), dimethyl sulfoxide, and isopropyl alcohol possess scavenging abilities towards photo-generated species such as $\bullet O_2^-$, h^+, e^-, and •OH radicals, respectively. In the absence of scavengers, the degradation of CP increases by 67% for OSFTC. The introduction of dimethyl sulfoxide into

the photo-reaction marginally enhances the degradation efficiency of the pharmaceutical waste contained within it. Notably, the addition of 10 mM of isopropyl alcohol to the reaction mixture containing a 20-ppm solution of harmful waste resulted in a significant reduction in degradation efficiency for the treatment of harmful waste, with reductions of up to 23%, 19%, for CP and PR respectively. Likewise, the efficiency decreased by up to 15% and 18% for CP with the addition of benzoquinone and EDTA, 19% and 23% for PR with the same additions. With dimethyl sulfoxide (DMSO), the reaction was quenched to 51% and 53% for CP respectively. In contrast, EDTA resulted in only minimal reduction in the reaction rates, with percentages of 61% and 59% for CP and PR respectively. This analysis suggests that hydroxyl radicals (•OH) and superoxide radicals ($\bullet O_2$) are primarily responsible for the removal of pharmaceutical pollutants. Through scavenging studies, it was confirmed that reactive oxygen species, particularly hydroxyl radicals (•OH) and superoxide radicals ($\bullet O_2$), are the primary contributors to efficient degradation, as opposed to the holes and electrons generated during the reaction.

3. Reusability of the OSFTC

The nanocomposite, in its initial state, demonstrates magnetic and catalytic characteristics, rendering it suitable for addressing carcinogenic pollutants and pharmaceutical waste. When selecting a catalyst for real-world usage, a crucial factor to consider is its durability and capacity for multiple uses. The nanocomposite was retrieved utilizing an external magnetic field i.e. with the help of magnet. The catalyst was positioned under the magnet, subjected to five washes with distilled water, dried, and subsequently employed in consecutive reactions. The nanocomposite's ability to be reused up to four times was clearly illustrated by the conversion or degradation percentage. The degradation efficiency remains consistent across numerous cycles for both toxic anthropogenic pollutant and pharmaceutical waste. Although a slight decrease in photocatalytic performance was observed after each cycle, in practical applications, even after undergoing four consecutive recycling runs, the nanocomposite's degrading efficiency remains nearly unchanged. The reusability assessment of the nanocomposite, depicted in Fig.S6 -b, plotted the degradation percentage against the number of cycles. Based on the results obtained, it can be affirmed that the nanocomposite is effective for pharmaceutical waste treatment and demonstrates satisfactory reusability in such applications. The reusability is facilitated by the inclusion of magnetite nanoparticles within the nanocomposite, allowing for the retrieval of the catalyst post-reaction using an external magnetic field, typically achieved using a magnet.

Optical Analysis of the OSFTC

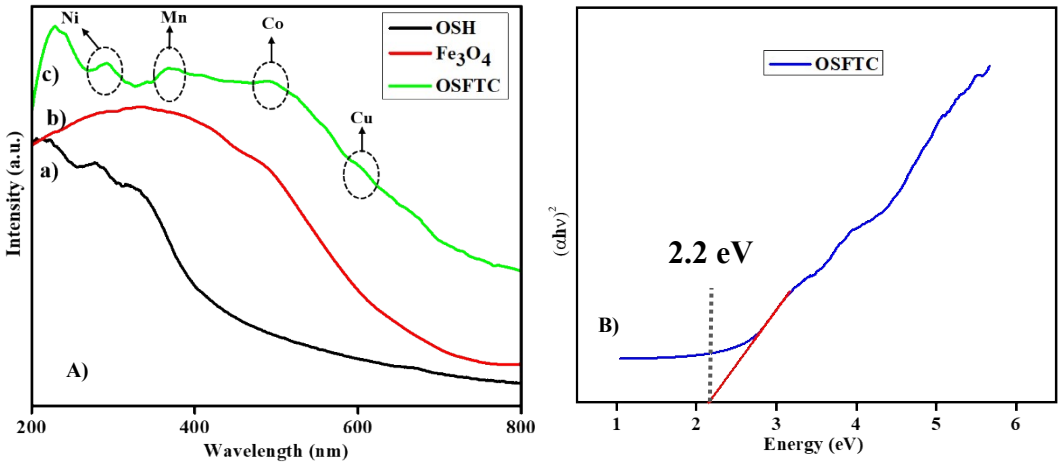

Fig. S1: Optical Analysis of the OSFTC – A) UV-visible plot for the OSFTC, B) Tauc's plot for the OSFTC.

XRD analysis

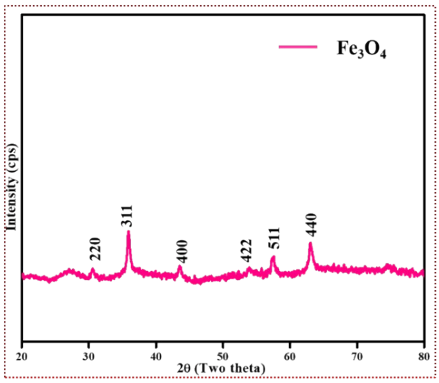

Fig.S2: XRD diffraction studies of the magnetite NPs.

3D-view analysis

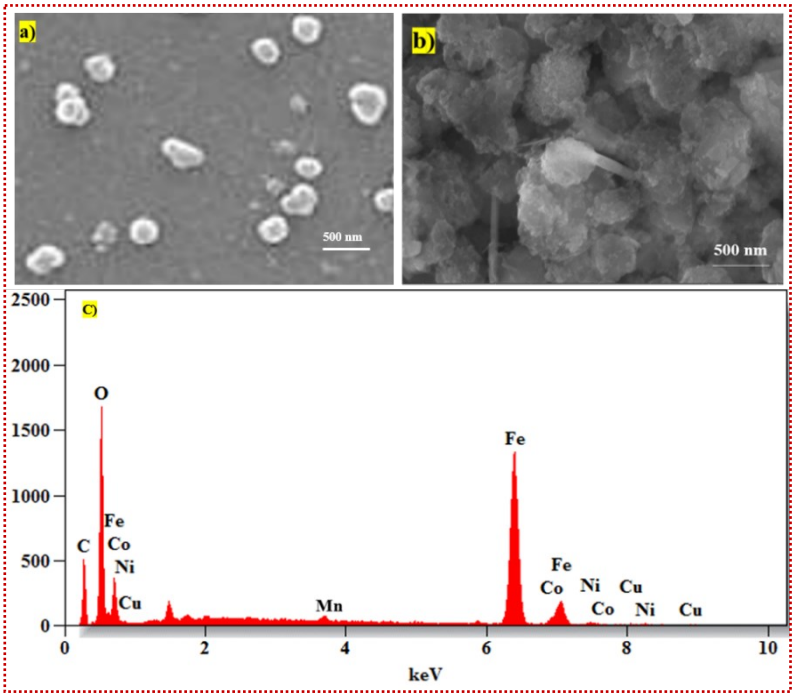

Fig.S3: SEM Analysis. a) SEM image of Fe_3O_4 NPs, b) SEM image of the OSFTC after the completion of the reaction and c) EDX pattern of the OSFTC.

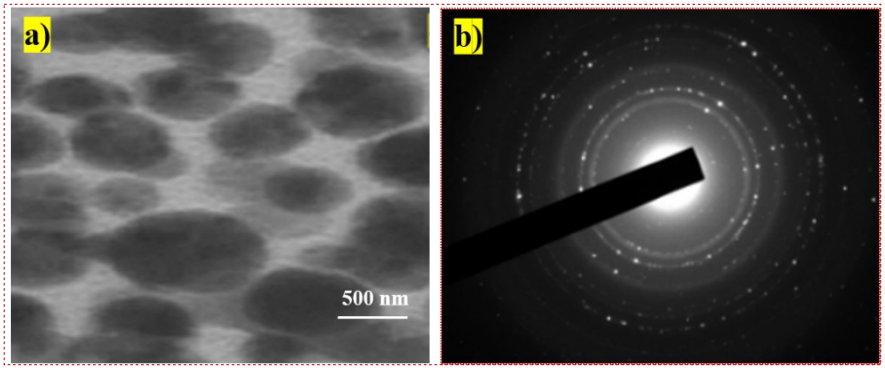

2D-view Analysis

Fig.S4: TEM analysis. a) TEM image of magnetite NPs and b) SAED pattern of the OSFTC.

Magnetic Nature Analysis

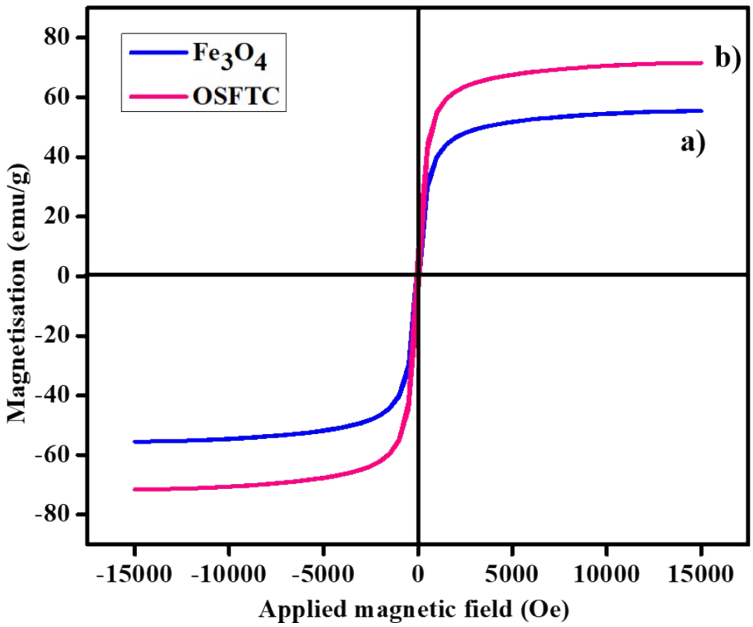

Fig.S5: VSM analysis of the OSFTC.

Reusability and Scavenger Analysis

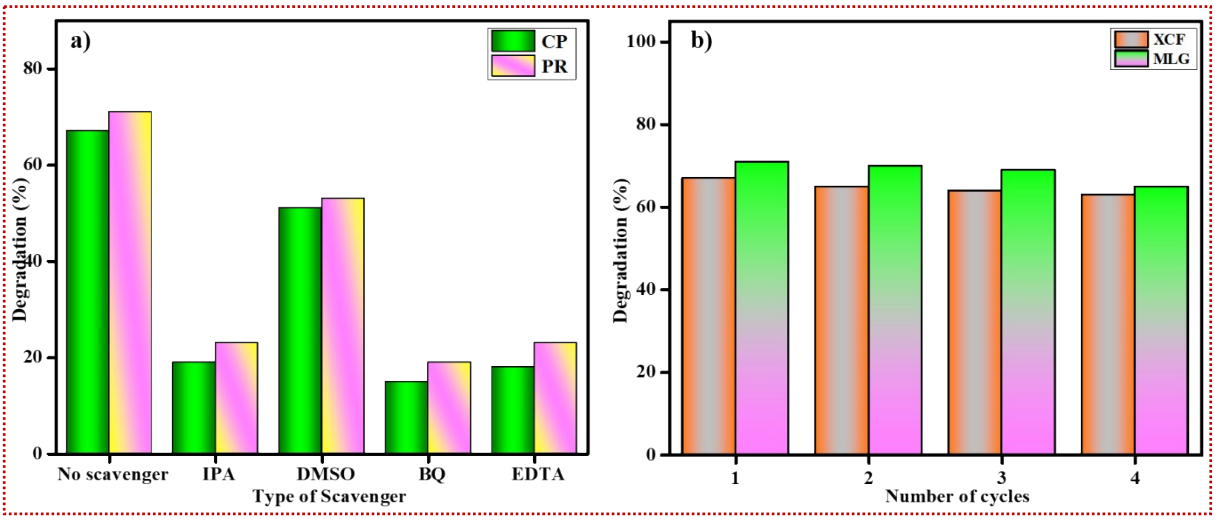

Fig. S6: a) Scavenger studies for the OSFTC and b) Reusability test for the OSFTC.

Point Zero Charge for CP

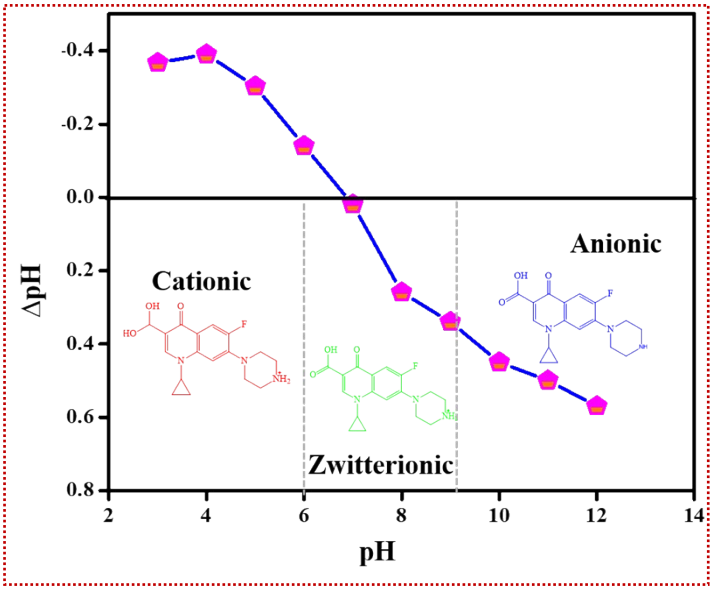

Fig. S7: Point-Zero Charge for CP (pH_{pzc}).

Elemental Composition of the OSFTC

Element	Net Counts	Weight %	Atom %	Atom % Error	Formula
C	2804	38.92	26.78	± 0.40	C
O	9443	28.98	47.42	± 0.63	O
Fe	20792	27.10	23.77	± 0.30	Fe
Co	415	1.35	0.60	± 0.12	Co
Ni	303	1.22	0.54	± 0.09	Ni
Cu	206	1.04	0.42	± 0.08	Cu
Mn	320	1.39	0.47	± 0.06	Mn
Total		100.00	100.00		

Fig. S8: Elemental composition for the as-crafted OSFTC.